THE JOURNAL OF PHYSICAL CHEMISTRY B

Article

pubs.acs.org/JPCB

Hybrid QM/MM Simulations of the Obelin Bioluminescence and Fluorescence Reveal an Unexpected Light Emitter

Shufeng Chen,[†,‡] Isabelle Navizet,[§,∥] Roland Lindh,[⊥,#] Yajun Liu,*[,†] and Nicolas Ferré*[,‡]

[†]Key Laboratory of Theoretical and Computational Photochemistry, Ministry of Education, College of Chemistry, Beijing Normal University, Beijing 100875, P.R. China

[‡]Aix-Marseille Université, CNRS, Institut de Chimie Radicalaire (UMR-7273), Marseille 13397, France

[§]Laboratoire de Modélisation et Simulation Multi Echelle, Université Paris-Est, MSME UMR 8208 CNRS. 5 bd Descartes, 77454 Marne-la-Vallé, France

[∥]Molecular Sciences Institute, School of Chemistry, University of the Witwatersrand, PO Wits, Johannesburg 2050, South Africa

[⊥]Department of Chemistry − Ångström, Uppsala University, P.O. Box 518, SE-751 20 Uppsala, Sweden

[#]Uppsala Center of Computational Chemistry - UC_3, Uppsala University, P.O. Box 518, SE-751 20 Uppsala, Sweden

Supporting Information

ABSTRACT: *Obelia longissima*, a tiny hydrozoan living in temperate and cold seas, features the Obelin photoprotein, which emits blue light. The Obelin bioluminescence and the Ca^{2+}-discharged Obelin fluorescence spectra show multimodal characteristics that are currently interpreted by the concomitant participation of several light emitters. Up to now, the coelenteramide luminophore is thought to exist in different protonation states, one of them engaged in an ion-pair with the nearby residue, His22. Using hybrid quantum mechanics/molecular mechanics (QM/MM) calculations, we demonstrate that such an ion-pair cannot exist as a stable light emitter. However, when His22 electric neutrality is maintained by means of another proton transfer, the phenolate state of coelenteramide exhibits emission properties in agreement with experiment. Finally, an alternative nonradiative decay pathway, involving the formation of a diradical excited state, is postulated for the first time.

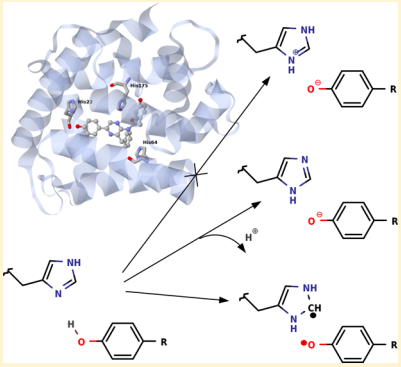

INTRODUCTION

Obelin proteins belong to the class of calcium-regulated photoproteins that exhibit bioluminescence (BL) whose intensity depends intimately on the amount of protein and on the presence of Ca^{2+} cations.[1,2] As such, Obelin and some of its mutants are mainly used to detect calcium in biological systems.[3] The BL chemical reaction involves the oxidative decarboxylation of the coelenterazine substrate in Obelin electronic ground state S_0, coupled to a nonadiabatic electronic transition toward the first singlet excited state S_1 and finally a radiative decay (Scheme 1).

Coelenterazine, although not covalently bound to the protein, is engaged in a relatively tight cavity and is in close contact with several residues (Figure 1) which in turn participate in the light emission efficiency and color modulation. Upon Ca^{2+} addition, Obelin substrate transforms to coelenteramide in an electronic excited state, leading to BL light emission, whose spectrum is mono- or bimodal (maximum wavelengths λ_{max} 400 and/or 475−495 nm in wild-type *Obelia longissima* and mutants).[4] The resulting photoprotein, Ca^{2+}-discharged Obelin, is also characterized by a strong fluorescence (FL) with λ_{max} about 510 nm.[5] Accordingly, and similar to other bioluminescent proteins,[6] the Obelin light emitter, i.e., the coelenteramide in S_1, is supposed to exist in different biomolecular states whose investigation is the main focus of this work.

Since the original mechanistic path proposed by McCapra and co-workers,[7,8] experimental and theoretical investigations have pointed out not less than six potential emitters that differ by their protonation states (neutral or anionic) and the site of deprotonation (phenolate, amide, ...)[4] Nevertheless, some of them have now been excluded;[9] therefore only two neutral forms (the chemiexcited one (**CS**) and **2H***) and the phenolate (**2O**$^-$*) in possible close contact with its countercation, hence forming an ion pair, are retained hereafter (see Scheme 1 for the labeling of the chemical structures). The currently admitted mechanistic pathway assumes **2H*** as being the first intermediate with light emission capabilities.[10] However, according to recent calculations performed in the gas phase, in various solvents, and in a model of the aequorin protein, the **CS** state is the first excited state intermediate in the chemiluminescence reaction.[11−13] Nevertheless, it is completely dark and only the next intermediate, **2H***, is associated with violet light emission, in agreement with experiment. Finally, via

Received: December 13, 2013
Revised: February 14, 2014
Published: March 6, 2014

Scheme 1. Bioluminescence Reaction Path Showing the Possible Light Emitters (Marked with *)

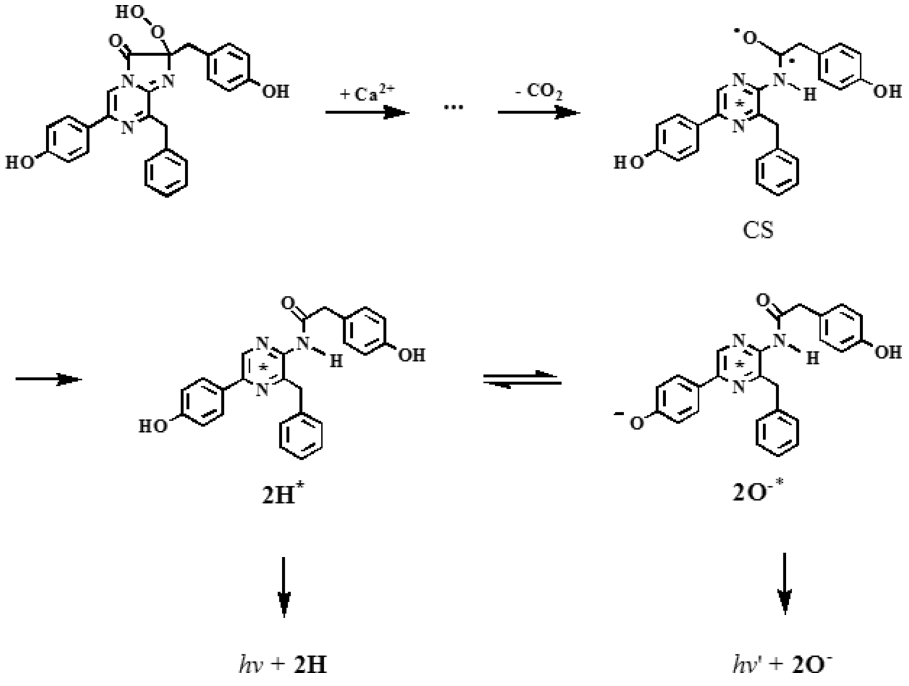

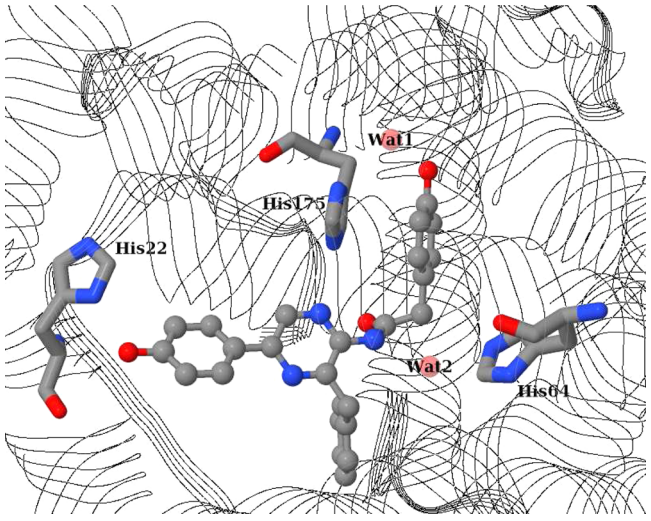

Figure 1. Schematic representation of Obelin (ruban), with coelenteramide in balls and sticks; histidine 22, 64, and 175 in sticks; and two water molecules in translucent balls. Hydrogen atoms are omitted for the sake of clarity.

excited state proton transfer, **2H*** transforms into **2O$^-$***, which emits the characteristic blue color of Obelin BL. This proton transfer, occurring on the picosecond time scale,[14] is possible due to the proximity of histidine His22 and the highest acidity of coelenteramide in S_1.[4] For this reason, **2O$^-$*** is usually assumed to form an ion pair with protonated His22.[15,16] Herein we report the results of a theoretical investigation of Obelin excited states by means of hybrid quantum mechanics/molecular mechanics (QM/MM) calculations,[17−21] which demonstrate unambiguously and for the first time that the *ion pair formed by* **2O$^-$*** *and the protonated His22 has to be excluded from the list of possible light emitters* in Obelin BL and FL. We also show that two close histidine residues are good candidates to accept the released proton, implying that the photoluminescence activity of Obelin may be accompanied by a complex proton transfer mechanism. In that respect, Obelin and GFP-type photoproteins show similarities.[22]

OBELIN BIOMOLECULAR STATES

The identification of the Obelin light emitters is based on the determination of low energy structures in S_1 whose vertical emission energies match the experimental λ_{max} values. Because these structures characterize both the luminophore and its close biological surroundings, we refer to them as biomolecular states in the following.

The stability of each biomolecular state characterizing the Obelin light emitter depends mainly on its origin (BL vs FL) and on the interactions between coelenteramide and the residues in the binding pocket. Most notably, the presence of His22, along with tryptophan Trp92, is involved in the deprotonation of coelenteramide neutral form (**2H***) to get **2O$^-$***,[15,23] which eventually emits light. Although ion pairs are short-lived in the gas phase, they can exist in a condensed phase thanks to stabilizing external factors. In the present case, these factors can be a strong electrostatic potential created by the coelenteramide surroundings and/or a loose cavity able to accommodate a weaker contact between **2O$^-$*** and His22. However, inspection of the available Obelin crystallographic structures[10,24] points to a tight and rigid cavity, a result confirmed by our calculations (see the discussion below). Hence it may be postulated that the proton transfer is more complex than the straightforward formation of the ion pair and may involve other proton acceptors. Among the large set of such acceptors available in the Obelin primary structure, we have focused on two histidine residues sufficiently close to coelenteramide. His175 (Figure 1) is supposed to be involved in the Obelin loop displacement upon Ca^{2+} accommodation that triggers Obelin photoactivity and to participate to the stabilization of the chemiluminescent product by means of important hydrogen bonds.[10] Recently, His175 was also suggested to be involved in the activation of Obelin and in

dx.doi.org/10.1021/jp412198w | J. Phys. Chem. B 2014, 118, 2896−2903

Table 1. Initial Protonation States and Geometric and Electronic Details Characterizing the Final Structures of All the Biomolecular Models

		starting protonation state				final structures				
		Coel	His22	His64	His175	R(O−H)[a]	R(N−H)[b]	R(O−N)[c]	charge[d]	e
BL	A	0	0	0	0	0.985	1.847	2.829	−0.08	**CS**
	B	0	0	0	0	0.989	1.833	2.820	−0.08	**2H***
	C	−1	+1	0	0	2.185	1.001	3.174	0.13	**2O$^{\bullet}$***
	D	−1	+1	+1	0	2.130	0.983	3.102	0.13	**2O$^{\bullet}$***
	E	−1	+1	0	+1	2.110	0.998	3.093	0.12	**2O$^{\bullet}$***
	F	−1	0	+1	0	1.831	1.030	2.852	−0.89	**2O^{-}***
	G	−1	0	0	+1	1.845	1.031	2.864	−0.90	**2O^{-}***
FL	B	0	0	0	0	0.987	1.849	2.835	−0.09	**2H***
	C	−1	+1	0	0	2.144	0.999	3.127	0.13	**2O$^{\bullet}$***
	D	−1	+1	+1	0	2.076	0.997	3.060	0.12	**2O$^{\bullet}$***
	E	−1	+1	0	+1	2.148	0.997	3.129	0.12	**2O$^{\bullet}$***
	F	−1	0	+1	0	1.858	1.029	2.883	−0.90	**2O^{-}***
	G	−1	0	0	+1	1.724	1.037	2.759	−0.88	**2O^{-}***

[a]Distance between coelenteramide phenol/phenolate oxygen and the labile proton, in Å. [b]Distance between His22 nitrogen δ and the labile proton; in Å. [c]Distance between His22 nitrogen δ and coelenteramide phenol/phenolate oxygen; in Å. [d]Mulliken charge carried by coelenteramide; in |e|. [e]See Scheme 1 and text for labeling.

Ca^{2+}-triggering of BL.[25] Another histidine (His64, Figure 1), together with a crystallographic water molecule, is thought to be a key residue during the decarboxylation process.[10]

Accordingly seven initial biomolecular states have been considered (hereafter labeled A to G). They differ by the protonation state of coelenteramide and of the three histidine residues His22, His64, and His175. These models are summarized in the left part of Table 1. The relative positions of these residues, together with coelenteramide and two crystallographic water molecules, are shown in Figure 1. More details regarding the hydrogen bond networks around coelenteramide are given in Figure S2 in the Supporting Information.

COMPUTATIONAL DETAILS

Our Obelin models for BL and FL are based on experimental crystallographic structures (PDB 1EL4[24] and 2F8P,[10] respectively). Although the latter corresponds to the final photoproduct when the BL process is over, the former corresponds to the structure of Obelin before it is triggered by Ca^{2+}. Accordingly, we assume that the conformational change reflected by the experimental 25 nm shift between Obelin BL and FL occurs after BL light emission. Details on the calculations are given in the Supporting Information. In short, hybrid QM/MM calculations have been performed using time-dependent density functional theory (TD DFT)[26] for the subsystem treated quantum mechanically (including at least the coelenteramide substrate and His22, as required for studying the proton transfer between them), whereas the remaining part of the biomolecular systems is qualitatively modeled using the amber99 forcefield,[27] in which special parameters have been added for coelenteramide. The electrostatic coupling between the two subsystems is achieved using the electrostatic potential fitted (ESPF) approach.[28] Minimum energy structures in S_1 have been obtained by geometry optimizations using the CAM-B3LYP exchange−correlation functional and the 6-31G(d,p) basis set. This level of theory has been validated in previous studies regarding coelenteramide in various solvents.[12] Starting geometries have been obtained by successive energy minimizations of 1EL4 and 2F8P models using amber99, keeping the protein backbone in its crystallographic structure, which is assumed to generate an averaged environment for coelenteramide. Relative energies of the optimized structures have been obtained by performing QM/MM energy calculations with coelenteramide, His22, His64, and His175 in the QM subsystem.

STRUCTURAL ANALYSIS

To characterize the final protonation of each biomolecular state, significant bond lengths and electronic structure informations are reported in Table 1. Similarly to our previous study of coelenteramide in solvents,[12] we have also used the three angles ω_1, ω_2, and ω_3 to characterize the relative orientations of the coelenteramide principal moieties (phenol/phenolate, p-hydroxyphenylacetamide, toluene) with respect to the central section (pyrazine) (Scheme 2), as well as the C−O distance and the θ angle to determine the hybridization of the amide carbon atom. These data are reported in Table 2.

Biomolecular state A has been considered only for BL and the corresponding structure shows the expected sp^3 hybridization at the amide center, hence demonstrating that the first

Scheme 2. Key Geometrical Parameters in the Structural Analysis of Coelenteramide[a]

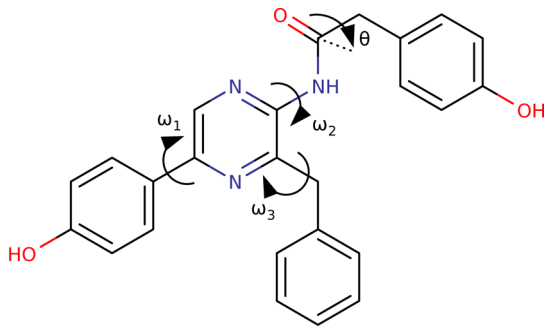

[a]ω_1, ω_2, and ω_3 refer to twisting angles of the external moieties (phenol/phenolate, p-hydroxyphenylacetamide, toluene) with respect to the central one (pyrazine). In the p-hydroxyphenylacetamide region, the θ angle characterizes the out-of-plane displacement of the amide C.

dx.doi.org/10.1021/jp412198w | J. Phys. Chem. B 2014, 118, 2896−2903

Table 2. Coelenteramide Structural Parameters (Angles in deg and Bond Lengths in Å)

		ω_1	ω_2	ω_3	θ	R(C−O)
BL	A	23	44	116	142	1.295
	B	17	58	117	−178	1.204
	C	21	53	119	−178	1.200
	D	23	54	118	−177	1.195
	E	20	39	121	−179	1.211
	F	25	51	108	−179	1.202
	G	21	37	120	−180	1.218
FL	B	23	73	83	−177	1.219
	C	24	65	84	−177	1.223
	D	27	67	80	−179	1.215
	E	30	74	79	−174	1.221
	F	37	65	80	179	1.216
	G	23	72	76	−175	1.229

intermediate in the Obelin BL process, **CS**, stays close to the reactant geometry, as already documented in a vacuum, solvent,[12] and aequorin,[13] a similar protein found in *Aequorea Victoria* jellyfishes. The other fully neutral state, B, corresponds to the **2H*** intermediate and shows similar geometrical and electronic structures in BL and FL, consistent with a neutral intermediate in both processes.

All the other biomolecular states feature a starting protonation state that shall lead to $\mathbf{2O^-}$* with the leaving proton transferred onto His22, His64, or His175. In the case of protonation on His22 (state C), we further considered the effect of having one of the other two histidine residues protonated at the same time (His22 and His64 in state D; His22 and His175 in state E). In these biomolecular states C, D, and E, the proton keeps its initial location on His22. However, it must already be mentioned that two (BL C and D) among the six final structures have been obtained from unconverged calculations. More precisely, and noteworthy for the following discussion, the corresponding DFT calculations did not converge due to a quasi-degeneracy between S_0 and S_1 (see the Supporting Information for details). Hence these two structures are not stable minima in S_1. In BL biomolecular state E and in FL states C, D, and E, the calculations ended normally; nevertheless, they also converged to a similar quasi-degeneracy of S_0 and S_1. Notice also that coelenteramide and His22 are pulled apart by 0.2−0.3 Å further than in the other biomolecular states (see R(N−O) in Table 1). This larger distance between coelenteramide and His22 can be rationalized by considering the modification of the coelenteramide electronic structure in these biomolecular states.

First, the Mulliken charge analysis (Table 1) reveals that coelenteramide carries ca. 0.1|e|, indicating a neutral electric charge. This result implies that the transfer of the proton from coelenteramide to His22 induces a simultaneous electron transfer. This unexpected result is confirmed by the analysis of the modification of the electronic density upon $S_0 \rightarrow S_1$ transition (Figure 2). Although the biomolecular state B exhibits a limited electronic redistribution strictly localized on coelenteramide, the biomolecular state C features a large increase of the electron density on His22 accompanied by a decrease on coelenteramide, a clear signature for an electron transfer between the two moieties. Hence the final electronic structures characterizing state C, as well as the D and E ones, does not correspond anymore to the initially hypothetized ion pair, but merely to a neutral diradical electronic state. For this

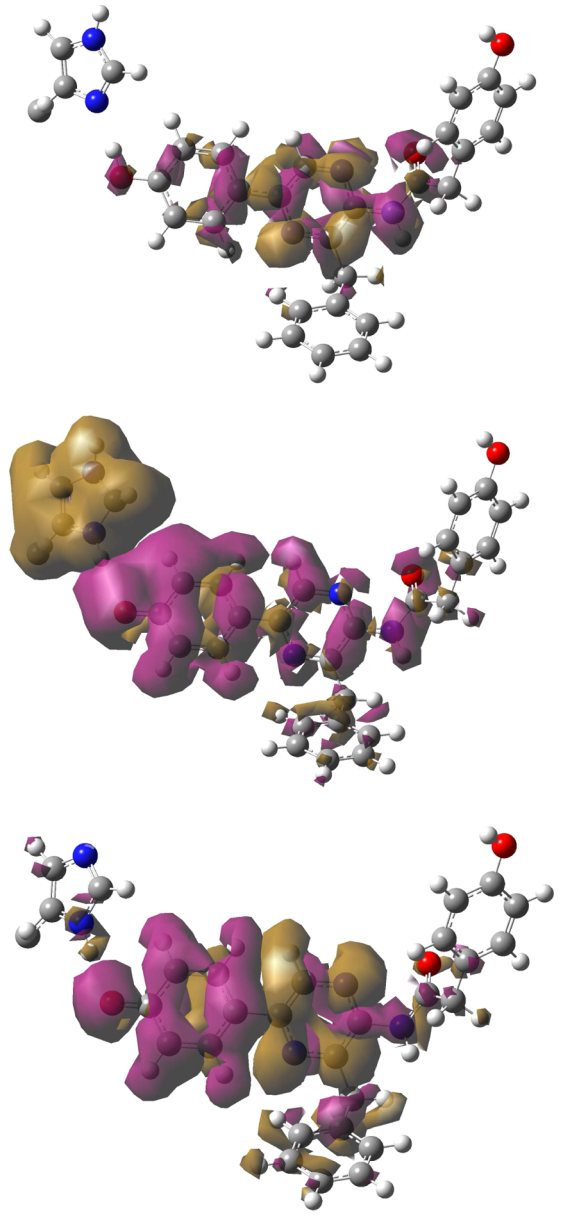

Figure 2. Electron density differences between S_0 and S_1 for BL biomolecular states B (top), C (middle), and G (bottom). Brown/purple surfaces surround regions characterized by an electron decrease/increase upon $S_1 \rightarrow S_0$ transition. The full set is available in the Supporting Information.

reason, the corresponding final electronic state of coelenteramide in biomolecular states C, D, and E is denoted $\mathbf{2O^{\bullet}}$* hereafter. It is noteworthy that, very recently, such a proton-coupled electron transfer[29] occurring in an excited state has been theoretically investigated by Hammes-Schiffer, in the case of *p*-nitrophenylphenol−methylamine complex in solution,[30] a system that can be seen as a minimal model of the coelenteramide−His22 assembly in Obelin.

The coelenteramide −1|e| formal charge is conserved only in the last two biomolecular states in which the leaving proton is hypothetized to reach His64 (F) or His175 (G). These states have been obtained by making the reasonable assumption that upon proton transfer from coelenteramide to histidine Nδ, the latter residue loses immediately the proton carried by Nϵ. Accordingly, His22 remains essentially neutral (only a small

dx.doi.org/10.1021/jp412198w | J. Phys. Chem. B 2014, 118, 2896−2903

Table 3. $S_1 \rightarrow S_0$ Vertical Emission Wavelengths (nm) (Oscillator Strengths in Parentheses) for All the Biomolecular States

			MM[a]	no MM[b]	no MM, no His22[c]	vacuum[d]
BL	A	**CS**	473 (0.00)	508 (0.00)	496 (0.00)	550 (0.00)
	B	**2H***	339 (0.39)	339 (0.42)	333 (0.38)	341 (0.34)
		exp	400			
	C, D, E	**2O$^{\bullet}$***	S_0/S_1 degeneracy			
	F	**2O$^-$***	498 (0.09)	491 (0.10)	569 (0.07)	890 (0.00)
	G	**2O$^-$***	504 (0.09)	510 (0.09)	593 (0.07)	890 (0.00)
		exp	485			
FL	B	**2H***	338 (0.24)	334 (0.30)	333 (0.22)	375 (0.05)
		exp	400			
	C, D, E	**2O$^{\bullet}$***	S_0/S_1 degeneracy			
	F	**2O$^-$***	533 (0.09)	526 (0.08)	623 (0.06)	910 (0.00)
	G	**2O$^-$***	492 (0.12)	478 (0.12)	557 (0.09)	958 (0.00)
		exp	509			

[a]Including electrostatic polarization of the QM subsystem by the MM one. [b]Excluding electrostatic polarization of the QM subsystem by the MM one, keeping the QM/MM geometry. [c]Excluding electrostatic polarization of the QM subsystem by the MM one, excluding the polarization due to His22, keeping the QM/MM geometry. [d]Gas phase geometry.

−0.1|e| charge is transferred from coelenteramide, Table 1) and forms an hydrogen bond with coelenteramide (histidine Nδ being the donor and coelenteramide phenolate O^- being the acceptor). BL and FL S_0 vs S_1 electron density differences displayed in Figure 2 show the same intramolecular charge transfer already documented in solvents.[12] These biomolecular states exhibit similar geometric features (notably a quite long N−H bond length, about 1.03 Å), clearly distinguishable from the other states considered in this study. Notice also, in FL state G, the closer contact between **2O$^-$*** and His22 (N···O distance is 2.76 Å whereas all the other ones are always larger than 2.82 Å). Together with the existence of **2O$^{\bullet}$***, the analysis of these geometric and electronic properties demonstrates that **2O$^-$*** can exist only in presence of a neutral His22. Hence the experimentally postulated ion-pair emitter does not find support in our theoretical simulations.

In our previous study of coelenteramide in the gas phase or implicit solvent models at the same level of theory,[12] various conformations have been obtained depending on the starting geometry or the photochemical process at work. Conversely, as shown in Table 2, the coelenteramide geometries optimized in the protein are all roughly similar, as far as BL or FL is distinguished. As expected for the first intermediate following the decarboxylation reaction in BL, only the biomolecular state A features a sp^3 hybridization in the amide moiety, as characterized by the longer C−O bond length and the pyramidalization at the carbon center. Now comparing BL biomolecular states and their FL counterparts highlights three main differences:

1. In FL, the twisting angle ω_1 (mean value = 27°) is always larger than or equal to its corresponding value in BL (mean value = 21°).
2. Similarly, the ω_2 angle is larger in FL (mean value = 70°) than in BL (mean value = 49°).
3. Conversely, the ω_3 angle is smaller in FL (mean value = 80°) than in BL (mean value = 117°).

These results illustrate how the coelenteramide conformation is modified during the Obelin BL process, as the result of the photoreaction but also because of the modification of the Obelin structure itself.

Another important result validates our initial assumption regarding the tightness of the cavity in which coelenteramide lies. Comparing the ω_1, ω_2, and ω_3 values to the ones previously found in less sterically hindered environments, we found that none of the conformations obtained in the present study matches the ones obtained in the gas phase or in the solvent.[12] For instance, **2H*** in the gas phase, benzene, or acetonitrile, always features a coplanar phenol/pyrazine conformation whereas in the protein both moieties are always tilted ($17 < \omega_1 < 37°$). The same difference holds for the other biomolecular states. An even more dramatic protein effect becomes apparent when ω_2 is considered. Although this angle was found to be negative in the gas phase or solvent,[12] it is always positive in the Obelin cavity. This is mainly due to the specific interactions between the phenol part of the *p*-hydroxyphenylacetamide moiety and the close amino acids, in particular His175. Conversely, the ω_3 values obtained in the protein are consistent with some of the conformations found in the gas phase or solvents.[12] This analysis points out the dramatic sterical effect induced by the protein on the coelenteramide conformation, an effect that is expected to have a noticeable impact on its light emission properties. Accordingly, the experimental analysis and rationalization of Obelin bioluminescence or Ca^{2+}-discharged Obelin FL by means of chemiluminescence of coelentaramide analogues in various solvents are expected to be weakly relevant.[16,31]

EMISSION ENERGIES

Computed vertical emission energies and experimental λ_{max} are reported in Table 3. First, it can be verified that the **CS** state in BL is dark. Second, the neutral form **2H*** (state B) is characterized by a ca. 340 nm vertical emission which, according to the expected 50 nm blue-shift already reported for TD DFT calculations,[12] is in correct agreement with the experimental expected λ_{max} (400 nm). As already mentioned, S_0 and S_1 are quasi-degenerate in each diradical state (C, D, and E). Any attempt to find a local minimum energy structure has been unsuccessful or eventually reached the neutral biomolecular state B, the proton transferring back to coelenteramide. Accordingly, these biomolecular states must be excluded from the list of possible BL or FL emitters. Now, BL states F and G show up as efficient emitters (oscillator strengths ≈0.1) at wavelengths (498 and 504 nm respectively) slightly red-shifted with respect to the experimental value λ_{max} (485 nm). It must be noted that the location of the proton (His64 or His175) has a negligible effect on the vertical emission energy (6 nm only).

dx.doi.org/10.1021/jp412198w | J. Phys. Chem. B 2014, 118, 2896−2903

In the case of FL, the same molecular states are characterized by efficient radiative decays with vertical emission wavelengths of 533 and 492 nm for F and G, respectively, hence bracketing the experimental λ_{max} = 509 nm value. The good agreement between the available experimental data and the calculated vertical emission energies for both BL and FL is a clear indication toward the participation of the F and G biomolecular states in these photochemical and photophysical processes in Obelin. As a further evidence, the experimental 24 nm red shift between **2O**$^-$* BL and FL λ_{max} can be satisfactorily reproduced considering either F or G states for BL, but only F in FL (with G, it would have led to a small blue shift, qualitatively inconsistent with experiment). Hence, this analysis suggests that the leaving proton may follow quite different transfer paths, depending on the initial driving force (BL or FL).

The principal effect of the protein (except for His22, His64, and His175) has been investigated by turning off the electrostatic potential felt by the QM subsystem, keeping the QM/MM final geometries. The larger difference (35 nm red shift) concerns the dark state A, whereas the other modifications are more limited (usually less than 10 nm), with the exception of state G in FL that exhibits a noticeable 14 nm blue shift in the absence of the protein electrostatic effect. In all, such a limited impact demonstrates that the emission properties of Obelin are mainly governed by the protonation state of coelenteramide and by the sterical hindrance imposed by the protein. As an illustration of the latter effect, the significant twist between the phenol/phenolate and pyrazine moieties induces a loss of π-conjugation, which is expected to lead to a red shift in the emission energies with respect to the coplanar situation. Indeed, when going from acetonitrile[12] to Obelin, the vertical emission wavelength for **2O**$^-$* increases from roughly 443−482 nm (depending on the considered conformer) to 492−533 nm. Hence, to further investigate the surrounding effects, we have complemented the previous results for **2H*** and **2O**$^-$* with new vertical emission energies of coelenteramide (i) in the absence of His22 and (ii) after geometry optimization in the gas phase. The results are reported in the last two columns in Table 3. Although the interactions with His22 modify the **CS** and **2H*** BL and FL energies only marginally (max 12 nm), they dramatically blue shift the **2O**$^-$* light emission (between 80 and 100 nm). Accordingly, His22 is significantly destabilizing the **2O**$^-$* excited state. Finally, reoptimizing the QM/MM geometries while eliminating all interactions with the surroundings leads to gas phase structures similar to the ones we already obtained[12] (structures available in the Supporting Information, Table S1). In particular, **2O**$^-$* BL and FL emission energies are strongly red-shifted, due to the complete loss of π-conjugation resulting from the final orthogonality between the phenolate and pyrazine moieties, with oscillator strengths close to zero.

In summary, if the BL and FL λ_{max} of Obelin are primarily determined by the protonation state of coelenteramide, they are tuned by the steric constraints imposed by the tight cavity (planarization and relative orientation of the coelenteramide moieties) and, to a lesser extent, by the electrostatic potential generated by the coelenteramide surroundings (especially His22). Moreover, the final location of the proton released by **2H*** leading to **2O**$^-$* does not seem to be of primary importance for what concerns the color of the emitted light.

QUALITATIVE BL AND FL PATHWAYS

Besides having demonstrated that the ion-pair cannot exist in S_1, we draw a *qualitative static* picture of both BL and FL processes in Obelin. Keeping in mind the nonequilibrium behavior inherent to these processes, the energetic comparison of the biomolecular states may give some hints about the most probable mechanistic pathway. For this purpose, the relative energies of the different biomolecular states (except D and E whose total protonation states are different) are reported in Figure 3.

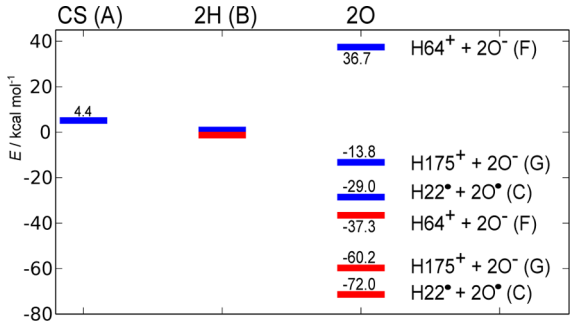

Figure 3. Relative energies of the biomolecular states (in parentheses, see text) in BL (blue) and FL (red). For comparison purposes, the QM/MM energies have been computed using coelenteramide and the three histidine residues as the QM subsystem (Table S2 in the Supporting Information). For the sake of clarity, the * labels have been droped.

The previously postulated BL pathway in S_1 is confirmed: **CS** → **2H*** → **2O**$^-$*. The first step involves a small decrease of energy corresponding to the sp^3 to sp^2 rehybridization of the coelenteramide carbon atom where the initial decarboxylation reaction occurs in S_0 before the system reaches S_1. In the second step, **2H*** transfers its proton to His22, which in turn releases another proton, keeping its electric neutrality. We hypothetize this proton can reach either His64 (biomolecular state F) or His175 (biomolecular state G). However, F can be immediatly excluded, because of its too high energy (more than 36 kcal mol^{-1}above B, even higher than A, the first intermediate). Owing to the even lower energy of biomolecular state C, the path leading to **2O**$^{\bullet}$* may be also populated, suggesting an alternative nonradiative decay to S_0, which would contribute to the lower BL quantum yield. Such a hypothesis would need a deeper investigation of the reaction path, probably using semiclassical molecular dynamics simulations performed on an accurate potential energy surface.

Similarly to BL, the photophysical path characterizing FL in Ca^{2+}-discharged Obelin is quite clear: S_0 → **2H*** → **2O**$^-$*. Although G is energetically more stable than F, we have already excluded G in FL (see the discussion above, regarding the λ_{max} red shift between BL and CL). As in the case of BL, the **2O**$^{\bullet}$* state, if mechanistically reachable, may also be populated significantly, hence lowering the FL quantum yield.

Finally, in the (unlikely) hypothesis in which only His64 and His175 could accept it, the leaving proton may transfer preferentially to His175 in BL whereas it would be more probably located in His64 in FL. This result is mostly useful to realize that proton transfer paths may be process-dependent, i.e., may differ in BL and FL. Obviously, the determination of the proton location is only preliminary and shall be refined by testing other hypothesis, e.g., other proton acceptors. As a

dx.doi.org/10.1021/jp412198w | J. Phys. Chem. B 2014, 118, 2896−2903

matter of fact, the proton transfer kinetics must be consistent with **2H*** and **2O$^-$*** lifetimes, the latter being estimated to 4 ns from time-resolved FL measurements.[14] Further extensive investigations will help to decipher the possible pathways, clearly beyond the scope of the present study.

CONCLUSION

In this work dealing with the origin of BL and FL in Obelin, we have shown that the existence of a coelenteramide−His22 ion pair is not supported by our QM/MM simulations. Alternatively, our results suggest that coelenteramide can exist as phenolate anion only if His22 remains neutral, implying a complex proton transfer occurring together with the formation of electronically excited coelenteramide. Among the potential proton acceptors located in the close vicinity of Obelin luminophore, His64 and His175 have been selected on the basis of their implication in other steps of Obelin BL. However, our calculations have shown that the final location of the proton is not important for what concerns the light emission. Nevertheless, a more systematic investigation of all the proton transfer paths starting at His22 will be required to elucidate what are the most probable acceptors.

A simple decomposition of the mechanisms responsible for the tuning of the emitted light has highlighted two main contributions: strong interactions with His22 and the steric constraint induced by the tightness of the cavity in which lies the luminophore. Electrostatic interactions with the protein, which global effect seems to be of minor importance, deserve a more thorough investigation, because selected mutations can dramatically change the BL characteristics.[32]

As a final note that opens new perspectives in the rationalization of the BL and FL quantum yields, the biomolecular state **2O$^{\bullet}$***, a diradical state resulting from a proton-coupled electron transfer[30] between coelenteramide and His22, appears to be an energetically favorable structure (Figure 3). The calculated near-degeneracy between S_0 and S_1 suggests an alternative nonradiative funnel that may be significanly populated in both BL and FL processes, involving nonadiabatic events like conical intersections. Actually, the side-chain ring in His22 is significantly puckered at the ε carbon atom, somehow similar to what was already documented for the conical intersections in the bare imidazole system.[33] Removing the interactions with the protein, hence keeping only **2O$^{\bullet}$*** and His22, does not lift the degeneracy (Table S3 in the Supporting Information). Accordingly, this proton-coupled electron transfer-based diradical state appears to be an intrinsic feature of this molecular assembly, which turns out to be largely unaffected by the steric and electrostatic constraints induced by Obelin. Further investigations, involving more sophisticated levels of theory,[34−36] will be needed to assess the relevance of this intriguing result. For instance, such a process could be quenched by stronger surrounding effects, like a polar/protic solvent, as already documented in DNA base pairs.[37,38]

ASSOCIATED CONTENT

Supporting Information

Molecular structures, computational details, analysis of the hydrogen bond networks around coelenteramide, electronic density differences, geometrical parameters for gas phase geometries, absolute energies and vertical emission energies of all the biomolecular states, Cartesian coordinates of the structures. This material is available free of charge via the Internet at http://pubs.acs.org/.

AUTHOR INFORMATION

Corresponding Authors

*Y. Liu: e-mail, yajun.liu@bnu.edu.cn.

*N. Ferré: e-mail, nicolas.ferre@univ-amu.fr.

Notes

The authors declare no competing financial interest.

ACKNOWLEDGMENTS

S.C., Y.L., and N.F. thank the PHC Cai Yuanpei program for funding (Project No. 23982SE). I.N. thanks NRF South-Africa and Wits University (SPARC) for funding. Y.L. thanks the National Natural Science Foundation of China for financial support (Grant Nos. 21073017, 21273021, and 21325312) and the Major State Basic Research Development Programs (Grant No. 2011CB808500).

REFERENCES

(1) Vysotski, E. S.; Lee, J. Ca^{2+}-Regulated Photoproteins: Structural Insight into the Bioluminescence Mechanism. *Acc. Chem. Res.* **2004**, *37*, 405−415.

(2) Vysotski, E. S.; Markova, S. V.; Frank, L. A. Calcium-regulated Photoproteins of Marine Coelenterates. *Proteins* **2006**, *40*, 355−367.

(3) Frank, L. A.; Borisova, V. V.; Markova, S. V.; Malikova, N. P.; Stepanyuk, G. A.; Vysotski, E. S. Violet and Greenish Photoprotein Obelin Mutants for Reporter Applications in Dual-color Assay. *Anal. Bioanal. Chem.* **2008**, *391*, 2891−2896.

(4) Belogurova, N. V.; Kudryasheva, N. S.; Alieva, R. R.; Sizykh, A. G. Spectral Components of Bioluminescence of Aequorin and Obelin. *J. Photochem. Photobiol., B* **2008**, *92*, 117−122.

(5) Belogurova, N. V. Discharged Photoprotein Obelin: Fluorescence Peculiarities. *J Photochem. Photobiol. B* **2010**, *101*, 103−108.

(6) Rebarz, M.; Kukovec, B.-M.; Maltsev, O. V.; Ruckebusch, C.; Hintermann, L.; Naumov, P.; Sliwa, M. Deciphering the Protonation and Tautomeric Equilibria of Firefly Oxyluciferin by Molecular Engineering and Multivariate Curve Resolution. *Chem. Sci.* **2013**, *4*, 3803−3809.

(7) McCapra, F.; Manning, M. J. Bioluminescence of Coelenterates: Chemiluminescent Model Compounds. *J. Chem. Soc., Chem. Commun.* **1973**, 467−468.

(8) McCapra, F. Review Lecture: The Chemistry of Bioluminescence. *Proc. R. Soc. Lond. B* **1982**, *215*, 247−272.

(9) Min, C.-g.; Li, Z.-s.; Ren, A.-m.; Zou, L.-y.; Guo, J.-f.; Goddard, J. D. The Fluorescent Properties of Coelenteramide, a Substrate of Aequorin and Obelin. *J. Photochem. Photobiol. A* **2013**, *251*, 182−188.

(10) Liu, Z.-J.; Stepanyuk, G. A.; Vysotski, E. S.; Lee, J.; Markova, S. V.; Malikova, N. P.; Wang, B.-C. Crystal Structure of Obelin after Ca-triggered Bioluminescence Suggests Neutral Coelenteramide as the Primary Excited State. *Proc. Natl. Acad. Sci. U. S. A.* **2006**, *103*, 2570−2575.

(11) Roca-Sanjuán, D.; Delcey, M. G.; Navizet, I.; Ferré, N.; Liu, Y.-J.; Lindh, R. Chemiluminescence and Fluorescence States of a Small Model for Coelenteramide and Cypridina Oxyluciferin: A CASSCF/CASPT2 Study. *J. Chem. Theory Comput.* **2011**, *7*, 4060−4069.

(12) Chen, S.-F.; Navizet, I.; Roca-Sanjuán, D.; Lindh, R.; Liu, Y.-J.; Ferré, N. Chemiluminescence of Coelenterazine and Fluorescence of Coelenteramide: A Systematic Theoretical Study. *J. Chem. Theory Comput.* **2012**, *8*, 2796−2807.

(13) Chen, S.-F.; Ferré, N.; Liu, Y.-J. QM/MM Study on the Light Emitters of Aequorin Chemiluminescence, Bioluminescence, and Fluorescence: A General Understanding of the Bioluminescence of Several Marine Organisms. *Chem.—Eur. J.* **2013**, *19*, 8466−8472.

(14) van Oort, B.; Eremeeva, E. V.; Koehorst, R. B. M.; Laptenok, S. P.; van Amerongen, H.; van Berkel, W. J. H.; Malikova, N. P.; Markova, S. V.; Vysotski, E. S.; Visser, A. J. W. G.; Lee, J. Picosecond Fluorescence Relaxation Spectroscopy of the Calcium-Discharged Photoproteins Aequorin and Obelin. *Biochemistry* **2009**, *48*, 10486−10491.

(15) Vysotski, E. S.; Liu, Z.-J.; Markova, S. V.; Blinks, J. R.; Deng, L.; Frank, L. A.; Herko, M.; Malikova, N. P.; Rose, J. P.; Wang, B.-C.; Lee, J. Violet Bioluminescence and Fast Kinetics from W92F Obelin: Structure-Based Proposals for the Bioluminescence Triggering and the Identification of the Emitting Species. *Biochemistry* **2003**, *42*, 6013−6024.
(16) Mori, K.; Maki, S.; Niwa, H.; Ikedab, H.; Hiranoa, T. Real Light Emitter in the Bioluminescence of the Calcium-activated Photoproteins Aequorin and Obelin: Light Emission from the Singlet-excited State of Coelenteramide Phenolate Anion in a Contact Ion Pair. *Appl. Phys. A: Mater. Sci. Process.* **2006**, *62*, 6272−6288.
(17) Warshel, A.; Levitt, M. Theoretical Studies of Enzyme Reactions: Dielectric, Electrostatic and Steric Stabilisation of the Carbonium Ion in the Reaction of Lysozyme. *J. Mol. Biol.* **1976**, *103*, 227−249.
(18) Field, M. J.; Bash, P. A.; Karplus, M. A Combined Quantum Mechanical and Molecular Mechanical Potential for Molecular Dynamics Simulations. *J. Comput. Chem.* **1990**, *11*, 700−733.
(19) Senn, H. M.; Thiel, W. QM/MM Methods for Biolomolecular Systems. *Angew. Chem., Int. Ed.* **2009**, *48*, 1198−1229.
(20) Elgabarty, H.; Schmieder, P.; Sebastiani, D. Unraveling the Existence of Dynamic Water Channels in Light-Harvesting Proteins: Alpha-C-phycocyanobilin in Vitro. *Chem. Sci.* **2013**, *4*, 755−763.
(21) Dong, G.; Shaik, S.; Lai, W. Oxygen Activation by Homoprotocatechuate 2,3-Dioxygenase: A QM/MM Study Reveals the Key Intermediates in the Activation Cycle. *Chem. Sci.* **2013**, *4*, 3624−3635.
(22) Seward, H. E.; Bagshaw, C. R. The Photochemistry of Fluorescent Proteins: Implications for their Biological Applications. *Chem. Soc. Rev.* **2009**, *38*, 2842−2851.
(23) Malikova, N. P.; Stepanyuka, G. A.; Franka, L. A.; Markova, S. V.; Vysotskia, E. S.; Leeb, J. Spectral Tuning of Obelin Bioluminescence by Mutations of Trp92. *Biochemistry* **2003**, *554*, 184−188.
(24) Liu, Z.-J.; Vysotski, E. S.; Chen, C.-J.; Rose, J. P.; Lee, J.; Wang, B.-C. Structure of the Ca^{2+} -regulated Photoprotein Obelin at 1.7 Å Resolution Determined Directly from its Sulfur Substructure. *Protein Sci.* **2000**, *3*, 2000.
(25) Eremeeva, E. V.; Natashin, P. V.; Song, L.; Zhou, Y.; van Berkel, W. J. H.; Liu, Z.-J.; Vysotski, E. S. Oxygen Activation of Apo-obelin-Coelenterazine Complex. *ChemBioChem* **2013**, *3*, 465−495.
(26) Casida, M. E.; Huix-Rotllant, M. In *Annual review of physical chemistry*; Johnson, M. A., Martinez, T. J., Eds.; Annual Review of Physical Chemistry BAI05; Annual Reviews, 2012; Vol. *63*; pp 287−323.
(27) Wang, J.; Cieplak, P.; Kollmann, P. How Well Does a Restrained Electrostatic Potential (RESP) Model Perform in Calculating Conformational eEergies of Organic and Biological Molecules? *J. Comput. Chem.* **2000**, *21*, 1049−1074.
(28) Ferré, N.; Ángyán, J. G. Approximate Electrostatic Interaction Operator for QM/MM Calculations. *Chem. Phys. Lett.* **2002**, *356*, 331−339.
(29) Weinberg, D. R.; Gagliardi, C. J.; Hull, J. F.; Murphy, C. F.; Kent, C. A.; Westlake, B. C.; Paul, A.; Ess, D. H.; McCafferty, D. G.; Meyer, T. J. Proton-Coupled Electron Transfer. *Chem. Rev.* **2012**, *112*, 4016−4093.
(30) Ko, C.; Solis, B. H.; Soudackov, A. V.; Hammes-Schiffer, S. Photoinduced Proton-Coupled Electron Transfer of Hydrogen-Bonded p-Nitrophenylphenol-Methylamine Complex in Solution. *J. Phys. Chem. B* **2013**, *117*, 316−325.
(31) Imai, Y.; Shibata, T.; Maki, S.; Niwa, H.; Ohashi, M.; Hirano, T. Fluorescence Properties of Phenolate Anions of Coelenteramide Analogues: The Light-emitter Structure in Aequorin Bioluminescence. *J. Photochem. Photobiol., A* **2001**, *146*, 95−107.
(32) Stepanyuk, G. A.; Golz, S.; Markova, S. V.; Frank, L. A.; Lee, J.; Vysotski, E. S. Interchange of Aequorin and Obelin Bioluminescence Color is Determined by Substitution of one Active Site Residue of each Photoprotein. *Biochemistry* **2005**, *579*, 1008−1014.
(33) Barbatti, M.; Lischka, H.; Salzmann, S.; Marian, C. M. UV Excitation and Radiationless Deactivation of Imidazole. *J. Chem. Phys.* **2009**, *130*, 034305.
(34) González, L.; Escudero, D.; Serrano-Andrés, L. Progress and Challenges in the Calculation of Electronic Excited States. *ChemPhysChem* **2012**, *13*, 28−51.
(35) Liu, Y.-J.; Roca-Sanjuan, D.; Lindh, R. Computational Photochemistry and Photophysics: The State of the Art. *Photochemistry* **2012**, *40*, 42−72.
(36) Auer, B.; Soudackov, A. V.; Hammes-Schiffer, S. Nonadiabatic Dynamics of Photoinduced Proton-Coupled Electron Transfer: Comparison of Explicit and Implicit Solvent Simulations. *J. Phys. Chem. B* **2012**, *116*, 7695−7708.
(37) Dargiewicz, M.; Biczysko, M.; Improta, R.; Barone, V. Solvent Effects on Electron-driven Proton-transfer Processes: Adenine-thymine Base Pairs. *Phys. Chem. Chem. Phys.* **2012**, *14*, 8981−8989.
(38) Kumar, A.; Sevilla, M. D. Excited State Proton-coupled Electron Transfer in 8-oxoG-C and 8-oxoG-A Base Pairs: A Time Dependent Density Functional Theory (TD-DFT) Study. *Photochem. Photobiol. Sci.* **2013**, *12*, 1328−1340.